

## Heterogeneous microstructures in oolitic carbonates

S. H. GUNDERSON<sup>1</sup> AND H. R. WENK

*Department of Geology and Geophysics  
University of California, Berkeley, California 94720*

### Abstract

Several bioclastic and oolitic carbonates have been studied with the transmission electron microscope. Aragonite has been distinguished from calcite on the basis of the SAD patterns and the morphology. The aragonite occurred either as microscopic crystals varying in length from 0.3 to 1 mm, or as larger masses twinned on {110}. It has been recognized in Pleistocene to Recent samples, but not in any of the Mesozoic or Paleozoic ages.

The study of the calcite in the Jurassic Twin Creek Oolite (Wisconsin) and other limestones with the TEM has revealed the presence of a modulated microstructure in low Mg calcite. The microstructure has two basic morphologies: one is a fine modulation with a wavelength of around 150Å; the other is coarser, with a wavelength of approximately 500Å. The modulations are not always distinctly planar, and occasionally they are superimposed upon each other. Both the coarse and fine modulations are found to be parallel to  $\{10\bar{1}4\} = r$ . The microstructure is similar in appearance and orientation to a structure found by Reeder (1980) in ancient calcian dolomites. No apparent chemical difference was found when comparing calcite crystals that have the microstructure to those that lack it.

The modulated microstructure was found to be rotated by *e* twins formed during deformation and is therefore older. It is suggested that the modulated structure is the result of an ordering phase transformation from a calcium carbonate in which the CO<sub>3</sub><sup>-</sup> groups are disordered, resulting in the formation of planar faults. Alternatively, defects and partial disorder developed during crystal growth. The substitution of cations such as magnesium, calcium, iron, or manganese would increase the likelihood of the formation of faults. This may explain why a similar microstructure is so pervasive in calcian dolomites. Disorder appears to occur in *secondary* calcite crystals, *i.e.*, those which formed by dissolution and reprecipitation from another carbonate.

### Introduction

Oolitic carbonates have been the subject of controversy and scrutiny in recent years. The nature of their mineralogy, fabric, origin, and diagenesis have all undergone considerable re-evaluation (Kahle, 1974; Sandberg, 1975; Bathurst, 1971; Wilkinson and Landing, 1978). Much of this is the result of Philip Sandberg's work on the Great Salt Lake ooids. Sandberg (1975) compared the mineralogy and fabric of Pleistocene to Recent oolites, especially to those of Mississippian age from the Central United States. Sandberg noted that the more recent ooids had originally been composed of tiny radial aragonite needles that had since altered to coarse neomorphic calcite, often with aragonite relics still included in the calcite.

This coarse calcite replacement of aragonite in both shells and ooids had been known for over 100 years (Sorby, 1879). However, the ancient ooids were not composed of coarse neomorphic calcite but rather retained a fine radial texture, as do the original calcite layers in shells. Sandberg concluded that the calcite found in ancient ooids was of primary origin rather than a secondary replacement of aragonite. He suggested that a progressive increase in the magnesium to calcium ratio in sea water over time resulted in favoring the precipitation of aragonite over calcite. This change of aragonite dominance over calcite is inferred to have occurred during early to middle Cenozoic time.

Much of Sandberg's work on ooids involved the use of the scanning electron microscope. The SEM was also widely used in oolite studies by such work-

<sup>1</sup> Present address: Mobil Oil Corporation, Denver, Colorado.

ers as Bathurst (1971) and Wilkinson and Landing (1978). However, ooids have never been studied in any detail using the transmission electron microscope (TEM). In this investigation, several oolitic carbonates were examined with the TEM (Table 1). All of the samples are believed to have formed at temperatures less than 50°C, and none of the carbonates are believed to have been submitted to high temperatures after diagenesis, although the Twin Creek limestone has undergone some low temperature deformation.

Transmission electron microscopy was done at 100 kV on a JEM 100C in the Department of Geology and Geophysics at Berkeley. This TEM is equipped with an energy dispersive X-ray analyzer (EDX), which allows for a compositional analysis of areas as small as 2000Å in diameter. TEM foils were prepared from thin sections of rock chips and thinned at 5 KV and 0.04 microamperes with argon gas. The thin foils were carbon coated prior to viewing with the microscope. In addition, some samples were analyzed with an ARL electron microprobe and an X-ray powder camera (Jagodzinski-type Guinier) for supportive evidence.

#### Identification of aragonite with the TEM

The identification of aragonite with the TEM was made by indexing selected area diffraction patterns (SAD). SADs were confirmed by comparing them to the SADs taken of aragonite single crystals. Some care must be taken because *h0l* diffraction patterns of calcite resemble aragonite due to double diffraction

with 003, a reflection which should be extinct, being strongly present. Aragonite in oolites was present either as large crystals twinned on {110} (Figure 1a) or as microscopic crystals occurring as randomly oriented inclusions in calcite and varying in length from 0.3 to 1 mm (Figure 1b). The Great Salt Lake oolite and the Pleistocene limestone from Big Pine Key, Florida, had significant amounts of aragonite in them. While X-ray powder diffraction of the Pleistocene Key Largo limestone from Florida did not indicate the presence of aragonite, TEM observations did show minute quantities of aragonite. The mineral does not have the same morphology as in the two other aragonite-rich samples and may therefore also be overlooked in SEM analyses. It is rather blocky in shape or has no distinct form. This is probably the result of extensive dissolution of the aragonite, leaving only small remnants in the calcite. Aragonite has not been found in the Jurassic or Mississippian limestones studied in this investigation (Table 1).

#### Modulated microstructure in calcite

The Giraffe Creek member of the Jurassic Twin Creek limestone consists of 60 to 70% ooids in a matrix of predominantly fine-grained calcite spar cement (Fig. 2). Most ooid nuclei are crinoid and mollusc fragments, the former originally high Mg-calcite, the latter aragonite. About one-fourth of the ooid nuclei are presently composed of sparry calcite crystals where fine details of the fossil fragments are lost. The shapes of these nuclei suggest that they are pelecypod debris, and Wilkinson and Landing (1978) conclude

Table 1. Sample of oolitic limestones studied in this investigation

Sample	Age	Formation and/or location	Aragonite present	Dolomite present	Modulated Microstructure	Percent of calcite	Percent of ooids
25-2	Pleistocene	Great Salt Lake, Utah	Yes	Yes	No	<10%	80%
215B-130	"	Big Pine Key, Florida	Yes	No	No	25-30%	75%
215B-131	"	Key Largo Limestones, Florida	Yes	No	Yes	40%	(50% fossil fragments and biosparite)
Jt-Series	Jurassic	Twin Creek, Wyoming	No	No	Yes	25%	60-70%
25-5-10	"	Limestones, Bath, England	No	No	Yes	30%	20% (50% fossil fragments)
25-5	Mississippian	St. Louis Limestone, Bowling Green, Kentucky	No	No	No	30%	70%
215B-130	"	St. Genevieve Limestone, Orange County, Indiana	No	No	No	30%	70%

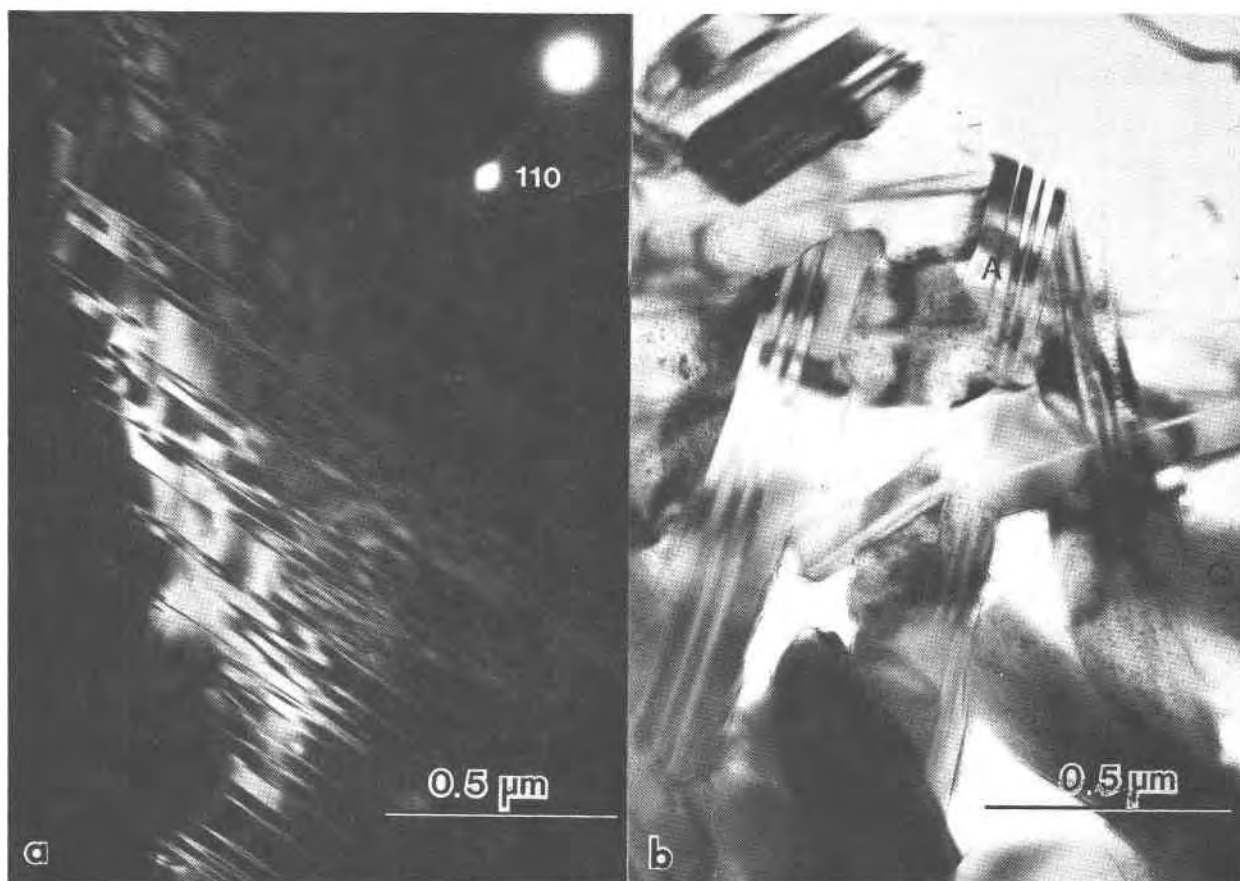


Fig. 1. Aragonite in oolitic limestone. (a) DF micrograph of twinning on  $\{110\}$  in aragonite of the Great Salt Lake Oolite.  $g = 110$ . SAD shows streaking along  $\{110\}$  perpendicular to the traces of the twins in the image; (b) Aragonite crystals with twinning on  $\{110\}$  (A) partially replaced by calcite (C) in limestone from Big Pine Key, Florida.

that such was originally aragonite that has since been replaced by secondary calcite. A few ooids have detrital quartz grains as nuclei. Occasionally the whole cortex is replaced by large crystals which display spherical outlines. But most ooid cortices consist of a very delicate radial fabric of calcite (Fig. 3a) which is believed by Wilkinson and Landing (1978) to be the result of primary growth (in accordance with Sandberg's 1975 suggestion). About 40% of the ooids have cortical coatings in which the detail has been obliterated by micritization. Examination of the cortical coatings with the TEM shows them to consist of many tightly compacted small grains on a scale of 0.2 μm (Fig. 3b). SADS of these tiny crystals display a polycrystalline pattern. Replacement fillings of probably mainly molluscan fragments are larger crystals, varying in size from 0.25 to 2 mm. They are generally twinned.

A heterogeneous microstructure has been discov-

ered in up to 75% of these larger crystals with the TEM. The structure which appears as a regular modulation is not always pervasive, as is seen in Figure 4a, where it is confined to a small central area. It is most easily observed at magnifications of 33 to 50 K. Images of the microstructure can be divided into two basic types. One type is a very dense, fine modulation, with a wavelength of approximately 150 Å and with a variation of plus or minus 50 Å (Fig. 4b). The second type consists of a broader coarse modulation (Fig. 4c). The coarse modulation tends to go in and out of contrast when tilting the specimen much more rapidly than the first type. It is generally more irregular and has a longer and more variable wavelength, averaging to 500 Å. The modulations are not necessarily strictly planar, but can be irregular. Occasionally, the two modulations are superimposed upon each other (cf., Fig. 9a).

Selected area diffraction patterns of the modulated

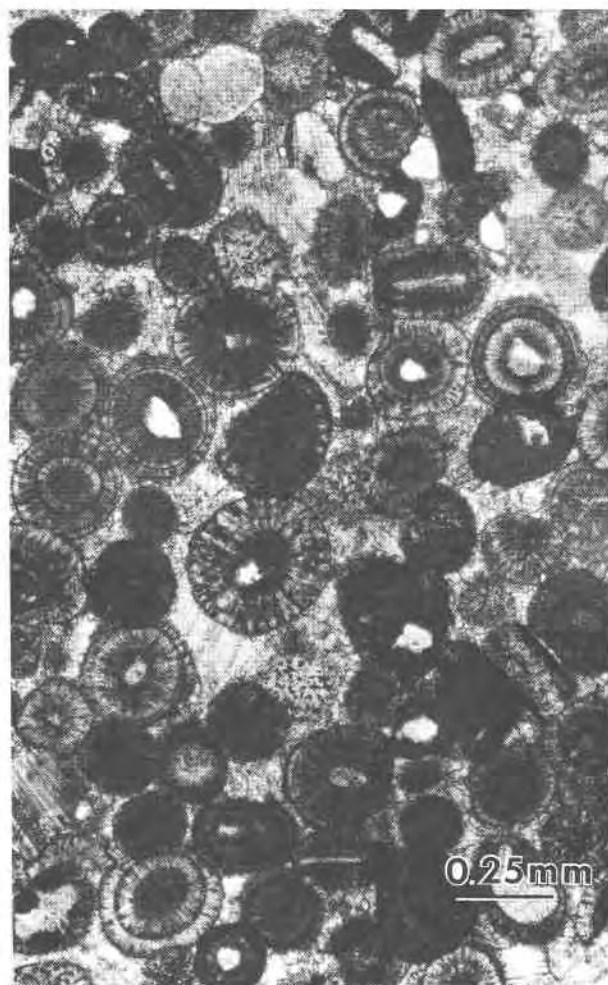


Fig. 2. Photograph of a thin section of the Giraffe Creek Member of the Twin Creek Limestone (Wyoming) showing ooids in a matrix of calcite spar cement. Notice pelecypod fragments, ooids replaced by large crystals, and frequent twinning in the large crystals and effects of pressure solution.

structure show a single reciprocal lattice without splitting of spots. Diffracted spots were occasionally broadened or streaked normal to the modulation (Fig. 4b), but streaking is rare and weak. It is most pronounced when the structure is viewed edge-on in the TEM. Also, very strongly exposed diffraction patterns show weak and diffuse "c" reflections, as discovered and defined by Reeder and Wenk, 1979, in calcian dolomite (insert to Fig. 4a). *c* reflections do not exist in the ideal calcite and dolomite structures. They occur halfway between spots in the  $01\bar{1}2$ ,  $10\bar{1}4$  and  $11\bar{2}0$  reciprocal directions, thus effectively doubling the *a* unit cell dimension. *c* reflections only occur in one of the three symmetrically equivalent orientations in the rhombohedral system and thus lower

the true symmetry to orthorhombic. No *c* reflections have been observed in calcite which lacks the microstructure.

#### Orientation of the modulated microstructure

In some cases crystals with the modulated microstructure are twinned (Fig. 5a and b). While tilting and rotating the specimen at a fixed position, a series of images and SAD micrographs were taken of these crystals. Images were first corrected for rotation, and then diffraction patterns and images were correlated and the traces of the twin plane (*t*), the fine modulated structure (*f*), and the coarse modulated structure (*c*) were plotted in stereographic projection relative to crystal coordinates (Fig. 6a and b). Dashed lines indicate the approximate orientation of the micrographs determined from SAD's. It could be five to ten degrees in error.

Plotting the traces of the twins shows that the twin plane is  $(\bar{1}018) = e$ . The fine modulation (*f*) is oriented parallel to  $(0\bar{1}14)$ , and the coarse modulation (*c*) parallel to  $(10\bar{1}4)$ . ( $\{10\bar{1}4\}$  is the cleavage rhomb *r* in calcite, using the crystallographic unit cell with  $c = 17\text{\AA}$ . Diffraction patterns cannot be indexed using the traditional morphologic unit cell with  $r = \{10\bar{1}1\}$ ). In Figure 6a, the specimen is tilted around an axis near  $[01\bar{1}7]$ , resulting in a greater spread in the traces of the twin and fine modulation. The axis of rotation in Figure 6b is  $[10\bar{1}1]$ . This axis permits the plotted traces of the coarse modulation (*c*) to be more spread out.

Twins along  $\{01\bar{1}8\}$  (*e* twins) are the common deformation twins in calcite (Mügge, 1889) which rotate the *c* axis  $52^\circ$  under application of a shear stress. Since  $(\bar{1}018) = e$ , is a rhombohedral plane, two forms of all other rhombohedral planes are converted into corresponding counterparts in host and twin.  $(\bar{1}104)$ , becomes  $(0\bar{1}14)_h$ , and  $(0\bar{1}14)_h$  becomes  $(\bar{1}104)_t$ . The third form,  $(10\bar{1}4)$ , attains a new orientation which does not coincide with a rational plane of the host. The topologic geometry undergoes changes as indicated by the switching of indices. The physical geometry of two forms of all rhombohedral planes, however, does not change, as illustrated in Figure 7.  $(0\bar{1}14)_h$  is the same plane as  $(\bar{1}104)_t$ , although it has changed its crystallographic identification.

Therefore, the fine modulation oriented along  $(0\bar{1}14)$  in the host will simply become the symmetrical  $(\bar{1}104)$  plane across the  $(\bar{1}018)$  twin plane, but there is no rotation of the modulated structure (Fig. 5b). On the other hand, the coarse modulation along  $(10\bar{1}4)$  is rotated by the twin (Fig. 5a and b).



Fig. 3. Cortex of ooids consisting of fine grained calcite in Twin Creek oolite. (a) Radial fabric of calcite needles with considerable preferred orientation as shown by the SAD; (b) Micritic calcite fabric of cortical coatings.

Twins in calcite from the Twin Creek oolite are believed to be the result of deformation. The fact that the modulation is rotated by the twin clearly indicates that it is older than the twin.

#### Darkfield imaging

During the course of this investigation, darkfield images were taken with different reflections (Fig. 8b through c), and significant variations in strength and detail of the modulations were observed. As mentioned previously, the coarse modulation goes in and out of contrast much more rapidly than the fine modulation. Strongest contrast of both modulations was generally obtained when  $g = 01\bar{1}4$ , and the modulations often appeared more continuous in this orientation. This is to be expected since the modulated structure is then viewed edge-on. Darkfield contrast in Figure 8 ranges from strong, when  $g = 10\bar{1}4$ , to moderate, when  $g = 11\bar{2}3$ . There is a reversal of contrast in the modulated structure when changing from brightfield to darkfield conditions (Fig. 8a, b). The microstructure in Figure 8 has sharp, distinct boundaries with fringes. Usually the boundaries are more diffuse. While there is variation in contrast, it is very

difficult to get the modulated structure out of contrast completely. Two beam contrast experiments are not compatible with  $\pi$  boundaries such as those with a displacement vector  $R = [2/3a_1 \ 1/3a_2 \ 1/6c]$  which is the most obvious vector in the calcite structure. The large number of fringes suggests stacking faults with short extinction distances rather than APB's, probably due to structural distortions and disorder of  $\text{CO}_3^{2-}$  groups. Because strong contrast is observed for  $g = 0006$ , the faults are also not stacking faults with  $R = [1/3a_2]$ , observed by Barber, *et al.* (1977), in deformed dolomite. Faults in Figure 8 are clearly planar, and we speculate that most of the regular modulation is due to planar defects associated with partial dislocations. Contrast analysis is complicated by the fact that a fair density of secondary dislocations produced during subsequent deformation is superposed on and unrelated to the modulated structure.

#### Discussion of the modulated microstructure

Modulated microstructures oriented along  $\{10\bar{1}4\}$  were also found in calcite in the Jurassic oolite from Bath, England, and the Key Largo limestone from

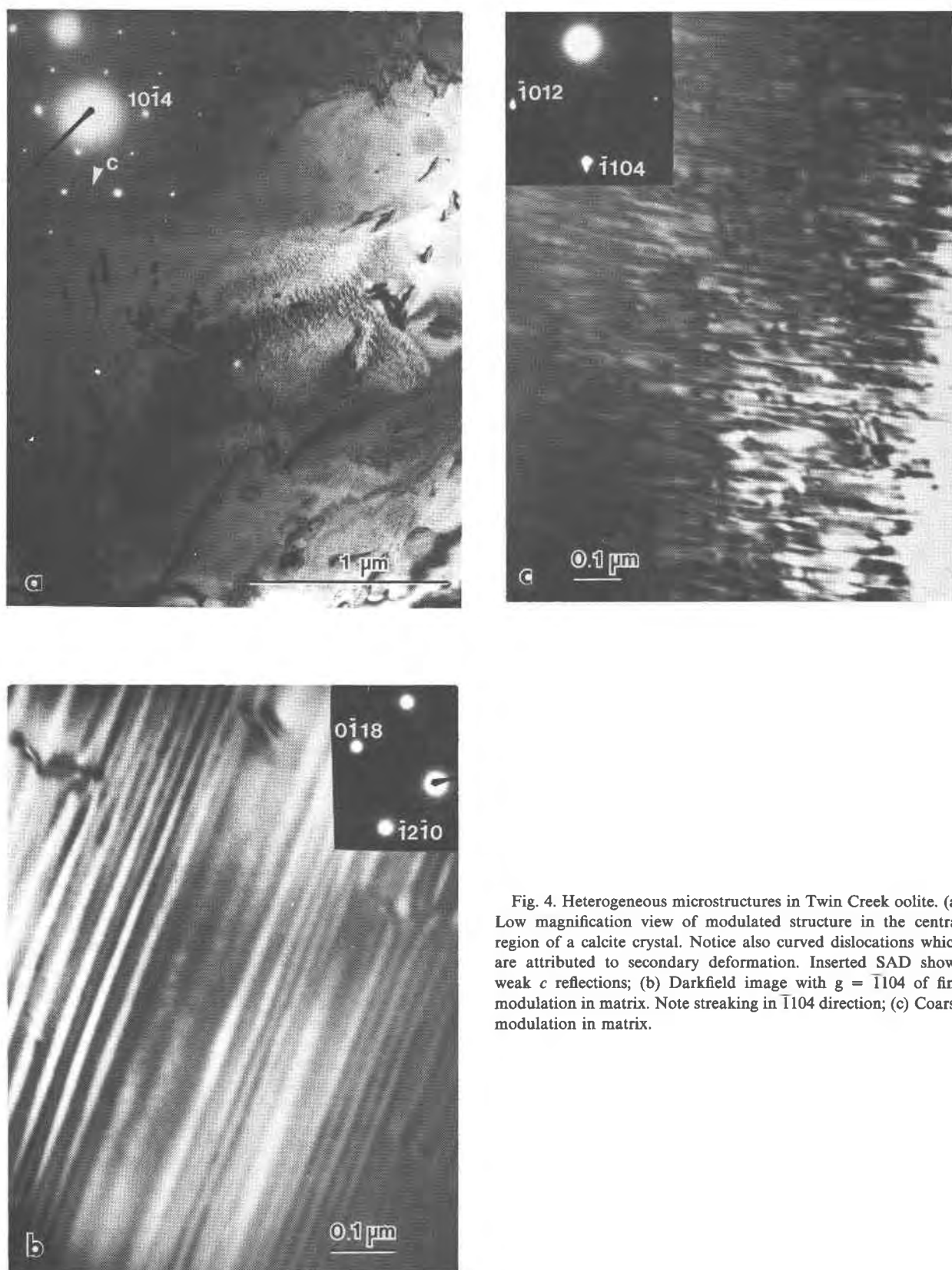


Fig. 4. Heterogeneous microstructures in Twin Creek oolite. (a) Low magnification view of modulated structure in the central region of a calcite crystal. Notice also curved dislocations which are attributed to secondary deformation. Inserted SAD shows weak  $c$  reflections; (b) Darkfield image with  $g = \bar{1}104$  of fine modulation in matrix. Note streaking in  $\bar{1}104$  direction; (c) Coarse modulation in matrix.

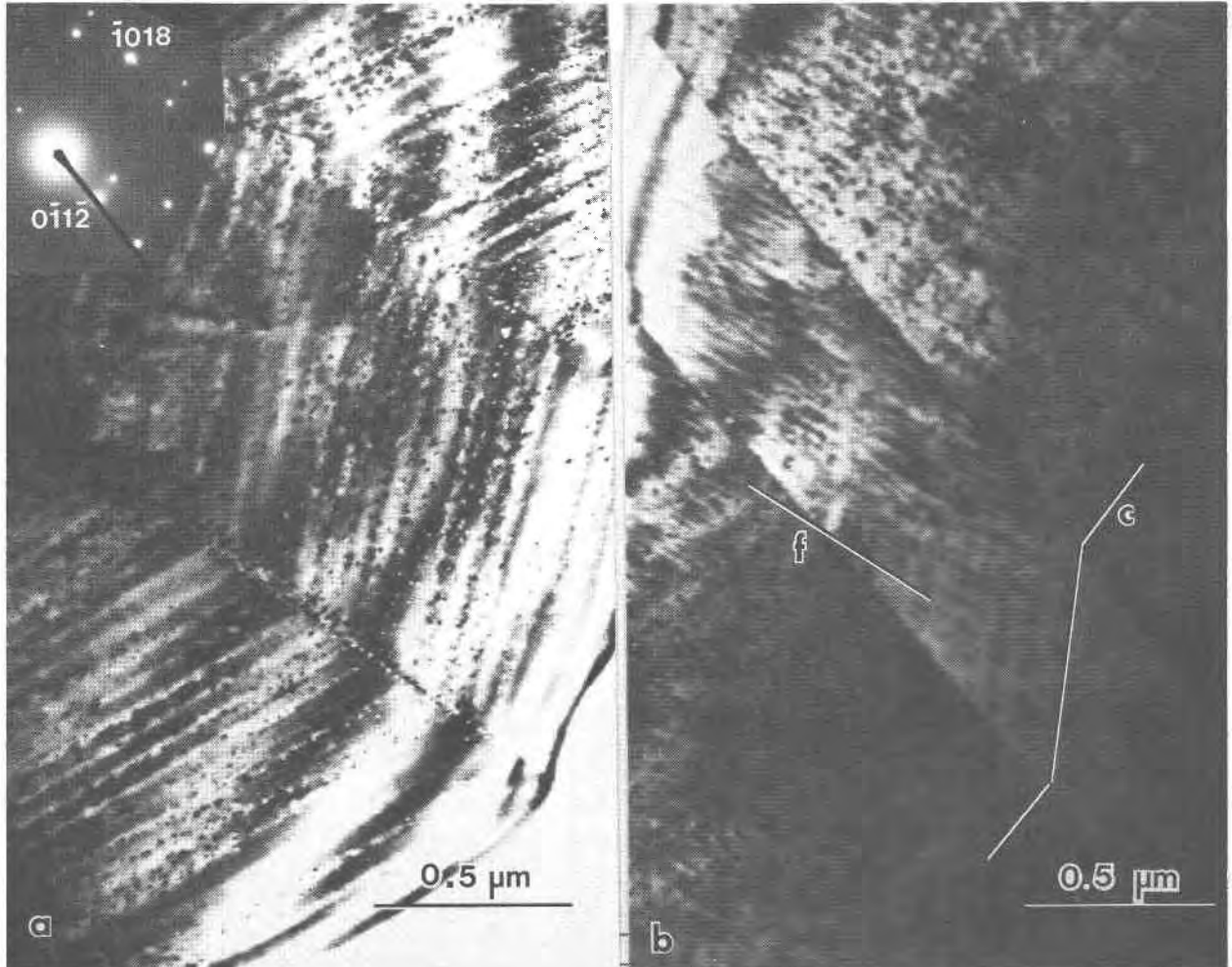


Fig. 5. Twinning in Twin Creek oolite. (a) Coarse  $(10\bar{1}4)$  modulation rotated by  $(\bar{1}018)$  *e*-twin. Fine spots are due to radiation damage; (b) Coarse  $(10\bar{1}4)$  modulation is rotated while fine  $(0\bar{1}14)$  modulation is not rotated by  $(\bar{1}018)$  twin.

Florida. The microstructures in the Key Largo calcite tended to be coarser and more diffuse than in the Bath, England, limestone (Gunderson, 1980). The modulation has not been found in calcite in the Pleistocene oolite from Big Pine Key nor in the Mississippian St. Louis and St. Genevieve oolites.

Of all of the samples investigated, the Twin Creek calcite has the most pervasive microstructure. This limestone was also the only one that was subjected to deformation. However, experimental studies of calcite deformation have not resulted in the formation of structural defects such as stacking faults along  $\{10\bar{1}4\}$  (e.g., Barber and Wenk, 1979; Goetze and Kohlstedt, 1977). Secondly, to attribute the modulated structure in the Twin Creek to deformation does not explain the presence of a modulated struc-

ture in the other limestones which are not believed to have undergone any deformation. *e* twins also rotate the modulated structure, indicating that the twins are younger than the modulated structure. The pattern of curved dislocations which are attributed to deformation (e.g., Fig. 4a) bears no relationship to the distinctly oriented modulation.

The modulated microstructure found in oolitic limestones is in many ways similar to the structures observed by Reeder and Wenk (1979) and Reeder (1980, 1981) in sedimentary calcian dolomites with about 5 mole percent excess  $\text{CaCO}_3$ . Figures 9b and 9d are TEM brightfield micrographs showing microstructures in Triassic calcian dolomites. Every variation in scale and morphology of modulations found in calcite has similar analogues in calcian dolomites,

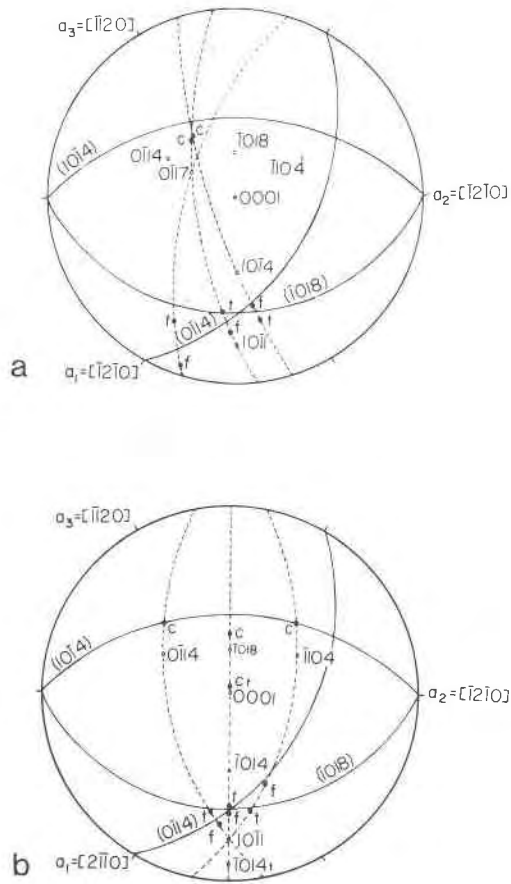


Fig. 6. Stereographic projections of twin and modulation geometry from trace analysis: *c* = trace of coarse modulation; *f* = trace of fine modulation; *t* = trace of twin; *c*<sub>1</sub> = trace of coarse modulation in twin. Coarse modulation is parallel to  $\{10\bar{1}4\}$ , fine modulation is parallel to  $\{0\bar{1}14\}$  and twin plane is  $\{1\bar{0}18\}$ .

although calcite is more heterogeneous, and different styles occur in the same sample, while in dolomite they are encountered in specimens of different localities, different ages, and different geological histories. Variations include coarse and fine modulations, modulations that are diffuse, those with single boundaries and distinct fringes, and two modulations superimposed upon each other. As in calcite, the structure in dolomite is also oriented parallel to  $\{10\bar{1}4\}$ . Reeder found this structure to be pervasive in most ancient calcian dolomites, but absent in recent ones. In both minerals *c* reflections have been observed in diffraction patterns in areas with heterogeneity.

Reeder and Wenk (1979) noted that the microstructure shows a striking resemblance to the "tweed structure" found in binary alloys which have decom-

posed into two different phases by a spinodal mechanism. In spinodal decomposition, the chemical composition of a crystal varies sinusoidally while the structure remains coherent (Champness and Lorimer, 1976). EDX microanalysis suggested heterogeneities in the Ca/Mg ratio, and Reeder (1980) concluded that the microstructure represented a compositional fluctuation in a coherent structure. Contrast in the image was explained to be primarily the result of strain in the lattice (Reeder, 1980) due to compositional differences.

EDX microanalysis of the calcite studied in this investigation shows no difference in chemical composition when comparing the areas with the modulated microstructure to that of homogeneous calcite. Microprobe analysis of the Twin Creek limestone proves that the rock is now entirely low magnesium calcite with negligible iron (Table 2), and the modulation in calcite cannot be the result of any Ca-Mg compositional fluctuation.

Lattice parameters refined from 15 reflections measured on X-ray Jagodzinski-type Guinier photographs of replacement calcite in which the modulated structure occurs are considerably shorter than those of micrite and microcrystalline ooids (Table 3). The lattice parameters of an Iceland spar quality single crystal of calcite ( $\text{MgCO}_3 < 0.1$  mole percent) was determined for comparison. Lattice parameter *a* of calcite replacement fillings would correspond to a

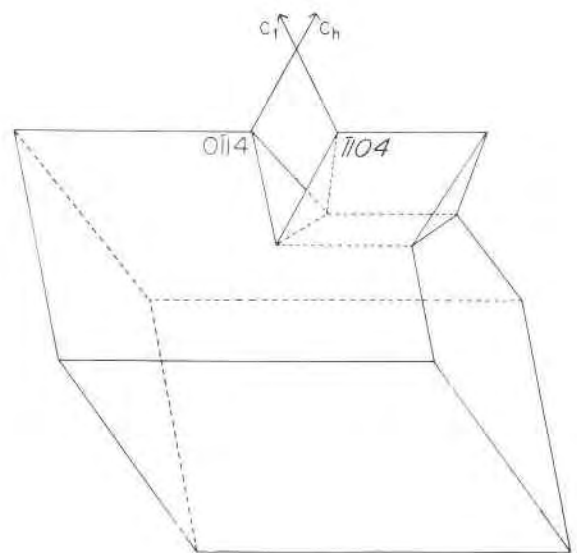


Fig. 7. Calcite cleavage rhomb with twin illustrating that the physical geometry of  $\{0\bar{1}14\}$  in the host is the same as  $\{1\bar{1}04\}$  in an *e*-twin, even though the *c*-axis has changed its orientation.



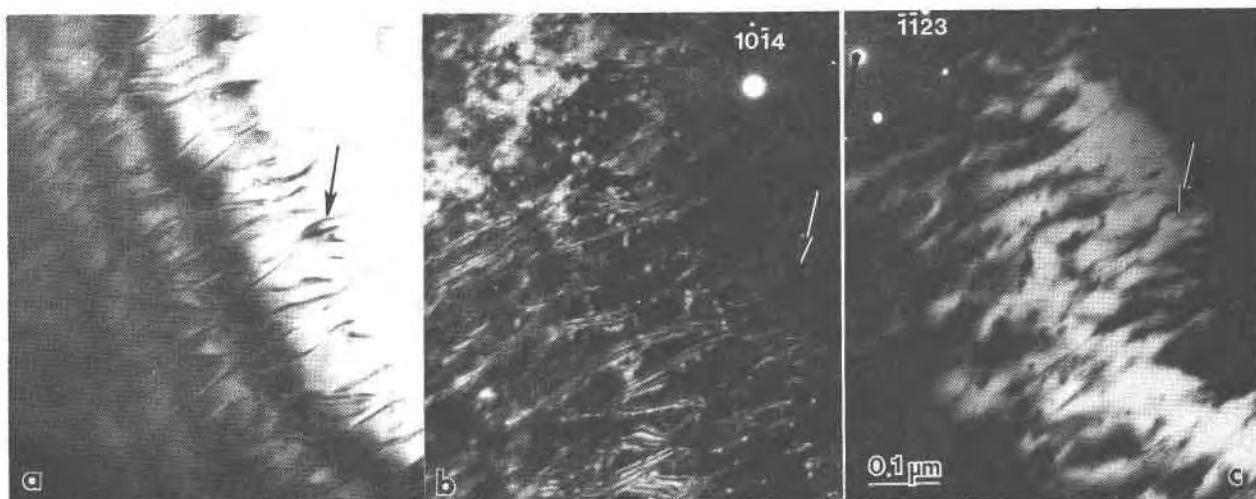


Fig. 8. Series of brightfield (BF) and darkfield (DF) micrographs of an exceptionally coarse modulation in Twin Creek Limestone. Arrows indicate same fringe in each micrograph. a-BF; b-DF  $g = 0\bar{1}4$ ; c-DF  $g = \bar{1}123$ .

calcite with 2.5 mole percent  $MgCO_3$  (Goldsmith and Graf, 1958) or with 3 mole percent  $FeCO_3$  (Graf, 1961) which clearly is not the case (Table 2). Yet there has to be a structural reason for the lattice distortion.

Some workers have discussed disorder in the anion layers of rhombohedral carbonates caused by rotation of the  $CO_3^{2-}$  groups (Lander, 1949; Lippman and Johns, 1969). In rhombohedral carbonates, the anions and cations occur in alternating planes perpendicular to the  $c$ -axis. All the anion groups of a given plane have the same orientation, but are rotated  $60^\circ$  with respect to the anions in the two adjacent planes.

The modulated structure could indeed be the result of rotational disorder of  $CO_3^{2-}$  groups. Sandberg (1975) suggests that replacement of aragonite by calcite occurs across a thin film of aqueous solution. Under such circumstances surface energy at the solution interface and the memory of the replaced carbonate counteract long range crystalline order within the newly formed calcite. As far as the nearest neighbor cations are concerned, the two orientations of  $CO_3^{2-}$  groups are equivalent. Differences are only apparent in the second neighbor anions. Thus it seems plausible that during rapid reprecipitation growth  $CO_3^{2-}$  groups attach in a partially or fully disordered arrangement, particularly if growth is mainly on  $\{10\bar{1}4\}$  faces.

Reeder (1980) disordered dolomite in heating experiments above  $1100^\circ C$ . Upon reordering, anti-

phase boundaries (APB's) (see, e.g., Amelinckx and Van Landuyt (1973), p. 73 for a definition) formed that have a displacement vector of  $R = [2/3a_1, 1/3a_2, 1/6c]$  corresponding to a translation of Ca into a Mg position. The same vector translates a  $CO_3^{2-}$  group in one orientation into one which is  $60^\circ$  rotated. Since APB's are observed and not  $c$ -twin boundaries, it follows that at these temperatures not only Ca-Mg but also  $CO_3$  are completely disordered (cf. discussion by Gratias *et al.*, 1979). In fact, by rapid quenching from  $1100^\circ C$ , partial substitutional disorder of Mg-Ca and rotational disorder of  $CO_3^{2-}$  can be preserved. It is generally accepted that the first phase of secondary dolomite to crystallize shows substitutional disorder (e.g., Berner, 1971). In analogy to high temperature observations it may also be accompanied by  $CO_3^{2-}$  disorder which cannot be detected in X-ray powder patterns. The latter applies equally to calcite.

The disordered carbonate is metastable. Given sufficient geologic time, dolomite attains an ordered arrangement of cations with alternating layers of Ca and Mg, thereby producing faults as discussed by Reeder (1981). Similarly, rotational disorder of  $CO_3^{2-}$  is likely to adjust. Since ordering takes place at large undercooling below the critical temperature ( $25^\circ C$  vs.  $1100^\circ C$ ), it proceeds by a continuous mechanism like that observed in intermediate plagioclase (e.g., Wenk and Nakajima, 1980), except that in calcite, ordering is positional and not substitutional. In the partially disordered state the structure contains large numbers of local defects, both linear and planar,

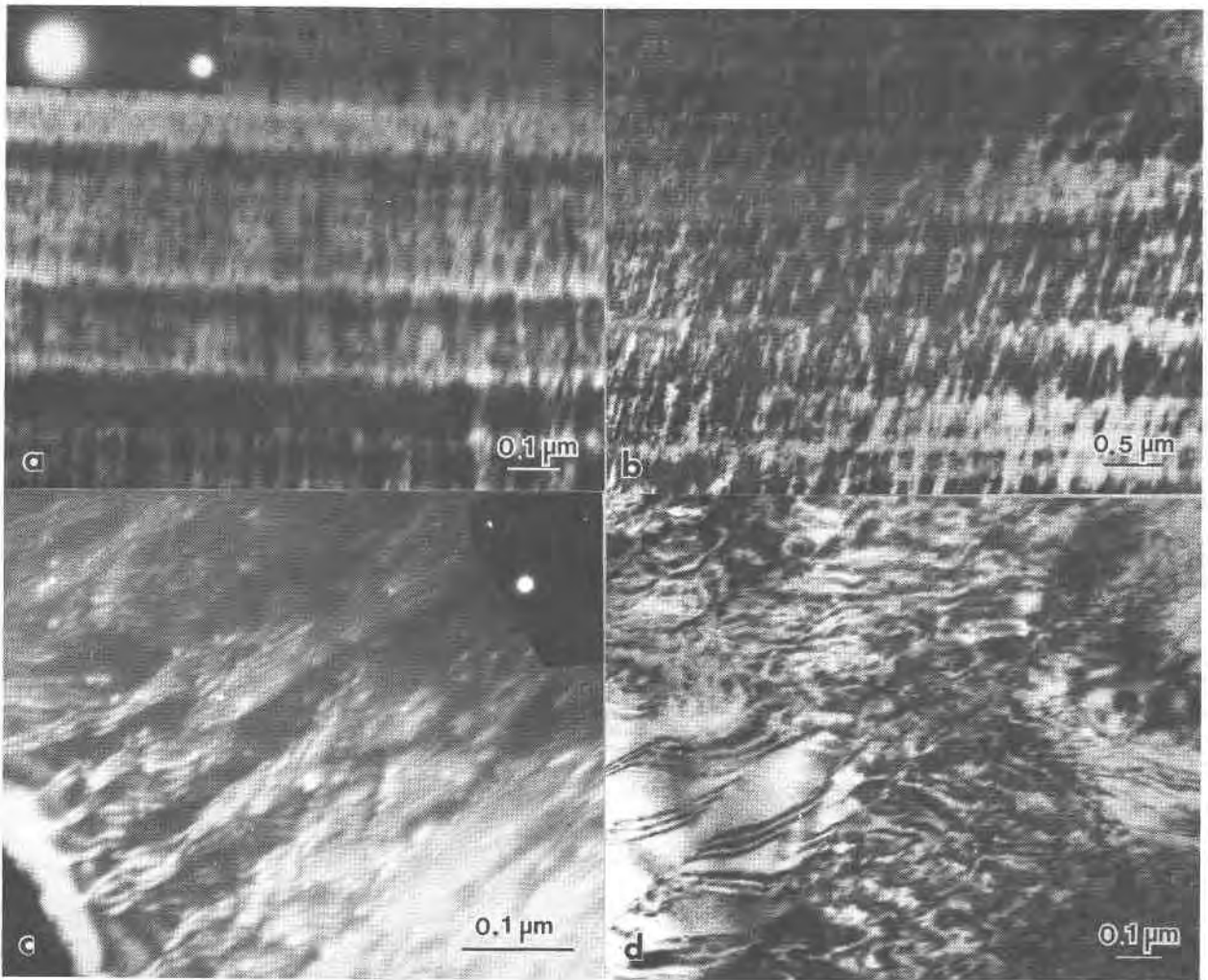


Fig. 9. Comparison of modulated microstructures in calcite and dolomite. (a) Superimposed coarse and fine modulation in Twin Creek oolitic limestone; (b) Superimposed coarse and fine modulations in calcian dolomites from the Triassic Dolomia Principale of N. Italy; (c) DF micrograph with  $g = 0\bar{1}14$  showing modulated structure with fringes terminated by partial dislocations; Twin Creek calcite; (d) BF micrograph of modulated microstructure in calcian dolomite of Triassic age from N. Jura Mountains, Switzerland, showing fringes terminated by partial dislocations.

which are difficult to characterize. If ordering goes to completion, domains are left behind, separated by APB's or twin boundaries.

Partial disorder and reversal of  $\text{CO}_3$  group orientations across  $\{10\bar{1}4\}$  interfaces could also be a direct result of growth under conditions of reprecipitation as described above and does not necessarily require a phase transformation.

There is good evidence for planar defects in cases where the structure has coarsened, such as in calcite (Fig. 9c) and in dolomite (Fig. 9d), and fringes delineating inclined faults are terminated by partial dislocations. In general, such coarsening is not very

common in the samples analyzed, and single faults cannot be resolved. As discussed above, contrast experiments are not conclusive and do not indicate simple  $\pi$  contrast as is required for APB's. Both observations are probably due to the fact that in calcite full order is rarely achieved and that strain (mainly rotational distortion of  $\text{CO}_3^{2-}$ ) is distributed over many unit cells, thereby producing intermediate stacking faults. Their orientation (*i.e.*, parallel to  $\{10\bar{1}4\}$ ) is such that the strain across the interface is minimized. But at least as a structural average the faults can be described as APB's. This is illustrated schematically in Figure 10. Note that the displacement vector is the

Table 2. Microprobe analyses of calcite in oolitic limestone from Twin Creek. Each value represents an average of 10 individual measurements

	Weight percent			Formula		
	CaO	MgO	FeO	Ca	Mg	Fe
ooid* (without microstructure)	51.81	0.71	0.43	0.978	0.013	0.008
spar crystals (with micro- structure)	53.93	0.37	0.48	0.984	0.009	0.007

\* Contains minor contamination of clays.

same as that observed by Reeder (1980, Figure 16) in heated and quenched dolomites.

The structural feature discussed so far only concerns the anion sublattice of calcite. However, it is likely that a chemical deviation from stoichiometry in the cation structure in calcian dolomites would enhance the probability for  $\text{CO}_3^-$  disorder. This could explain why the modulated microstructure is so pervasive. Reeder (1981) has provided convincing arguments that a chemical modulation exists in calcian dolomites, even though there it may also be combined with anion disorder. In fact,  $c$ -reflections could be indicative of the  $\text{CO}_3^-$  arrangement. In the region across faults such as those shown in Figure 10, the  $a$  cell parameter is doubled, and if such regions exist in sufficient volume, there may be coherent diffraction contrast (compare also Fig. 3, in Reeder and Wenk, 1979).

There are distinct differences between calcite and dolomite. In calcite, streaking in the diffraction pattern is subordinate, while it is pervasive in dolomite, indicating larger deviations from coherency in dolomite. The microstructure goes out of contrast much more easily in calcite, particularly with  $a$  reflections which have a small intensity contribution from oxygen. In dolomite, contrast is partially caused by scattering factor differences between Mg and Ca which apply equally to all reflections. The proposed model

Table 3. Lattice parameters of calcite determined from Jagodzinski-type Guinier photographs, Fe  $K\alpha_1$  radiation. (Error in parentheses.)

Sample	a (Å)	c (Å)
Accepted Standard*	4.9900	17.061
Twin Creek ooids	4.9875 (.0005)	17.047 (.006)
Twin Creek replacement crystals	4.9800 (.0006)	17.031 (.005)
Calcite single crystal, Chihuahua	4.9911 (.0006)	17.066 (.008)

\* Taken from Joint Committee Powder Diffraction File, 1974.

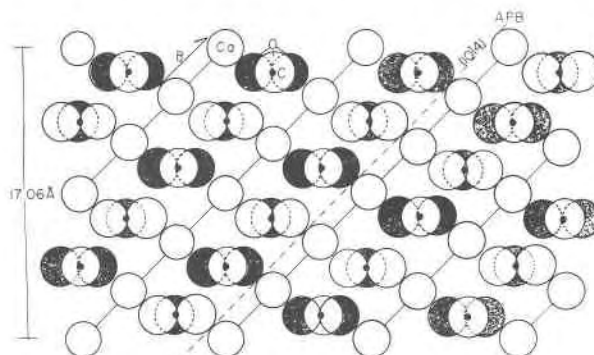


Fig. 10. Schematic model of calcite showing a section through a  $(\bar{1}2\bar{1}0)$  plane. The  $c$  unit cell dimension is indicated (17.61 Å). Calcium atoms are open circles; carbon atoms are black circles, and oxygen atoms are grouped with the atoms in the background shaded. The antiphase boundary (APB) results from a displacement  $R$  in the  $(10\bar{1}4)$  plane.

for anion disorder in calcite is based on circumstantial evidence and hence may have to be revised. It clearly needs to be corroborated by rigorous X-ray structure refinement which seems feasible for the large replacement spar crystals.

The reason for the presence of this modulated structure in certain oolitic or bioclastic limestones and the absence of it in others is uncertain. It appears to be found only where the calcite has replaced pre-existing aragonite. The chances for disorder are greater during secondary cementation or after the aragonite has been replaced by calcite during diagenesis with rapid crystallization. It is interesting to note that the calcian dolomites that have microstructure are also believed to be secondary (Reeder, 1980).

The new findings of heterogeneity in sedimentary carbonates call for a detailed reinvestigation of these minerals. The TEM, which allows probing of structural features on a very small scale and provides information on morphology, chemical composition, and a diffraction pattern, proves to be an instrument of great potential in sedimentological research. More limestones need to be studied with TEM to ascertain geological conditions for the occurrence of the heterogeneous microstructure and its petrological significance. Interestingly, similar structures have recently been observed in carbonatites (Wenk, Barber and Reeder, in preparation), supporting the hypothesis of structural disorder.

### Acknowledgments

Discussions with R. J. Reeder and M. Tucker, and a prompt review and editing by H. Green and K. Towe have been extremely valuable and helpful. Support from NSF grant EAR 78-23848 is appreciated.

## References

- Amelinckx, L. and Van Landuyt, J. (1976) Contrast effects at planar interfaces. In H.-R. Wenk, Ed., *Electron Microscopy in Mineralogy*, p. 68–112. Springer-Verlag, New York.
- Barber, D. J., Heard, H. C., Paterson, M. S., and Wenk, H. R. (1977) Stacking faults in dolomite. *Nature*, 269, 789–790.
- Barber, D. J. and Wenk, H.-R. (1979) Geological aspects of calcite microstructure. *Tectonophysics* 54, 45–60.
- Bathurst, R. G. C. (1971) *Carbonate Sediments and Their Diagenesis*. Elsevier, Amsterdam.
- Berner, R. A. (1971) *Principles of Chemical Sedimentology*. McGraw-Hill, New York.
- Champness, P. E. and Lorimer, G. W. (1976) Exsolution in Silicates. In H.-R. Wenk, Ed., *Electron Microscopy in Mineralogy*, p. 174–204, Springer-Verlag, New York.
- Goetze, C., and Kohlstedt, D. L. (1977) The dislocation structure of experimentally deformed marble. *Contributions to Mineralogy and Petrology*, 59, 293–306.
- Goldsmith, J. R. and Graf, D. L. (1958) Relation between lattice constants and composition of the Ca-Mg carbonates. *American Mineralogist*, 43, 84–101.
- Graf, D. L. (1961) Crystallographic tables for rhombohedral carbonates. *American Mineralogist*, 46, 1283–1316.
- Gratias, D., Portier, R., Fayard, M. and Guymont, M. (1979) Crystallographic description of coincidence-site lattice interfaces in homogeneous crystals. *Acta Crystallographica A* 35, 885–894.
- Gunderson, S. H. (1980) *Microstructures in Oolitic Carbonates*. MS Thesis, University of California, Berkeley.
- Kahle, C. F. (1974) Ooids from Great Salt Lake, Utah, as an analogue for the genesis and diagenesis of ooids in marine limestones. *Journal of Sedimentary Petrology*, 44, 30–39.
- Kitano, Y. and Kanamori, N. (1966) Synthesis of magnesian calcite at low temperatures and pressures. *Geochemical Journal*, 1, 1–10.
- Lander, J. J. (1949) Polymorphism and anion rotational disorder in the alkaline earth carbonates. *Journal of Chemical Physics*, 17, 892–901.
- Lippman, F. and Johns, W. D. (1969) Regular interstratification in rhombohedral carbonates and layer silicates. *Neues Jahrbuch für Mineralogie, Monatshefte* 5, 212–221.
- Reeder, R. J. (1980) *Phase Transformations in Dolomite*. Ph.D. Thesis, University of California, Berkeley.
- Reeder, R. J. (1981) Electron optical study of modulated microstructures in calcian dolomites. *Contributions to Mineralogy and Petrology* (in press).
- Reeder, R. J. and Wenk, H.-R. (1979) Microstructures in low temperature dolomites. *Geophysical Research Letters*, 6, 77–80.
- Sandberg, P. A. (1975) New interpretations of Great Salt Lake ooids and of ancient nonskeletal carbonate mineralogy. *Sedimentology*, 22, 497–537.
- Sorby, H. C. (1879) The structure and origin of limestones. *Geological Society of London, Proceedings*, 35, 56–95.
- Wenk, H. R. and Nakajima, Y. (1980) Structure, formation, and decomposition of APBs in calcic plagioclase. *Physics and Chemistry of Minerals*, 6, 169–186.
- Wilkinson, B. H. and Landing, E. (1978) "Eggshell diagenesis" and primary radial fabric in calcite ooids. *Journal of Sedimentary Petrology*, 48, 1129–1138.

*Manuscript received, December 22, 1980;  
accepted for publication, February 27, 1981.*